Biophysical Journal
Article

Biophysical Society

Cortical tension initiates the positive feedback loop between cadherin and F-actin

Qilin Yu,[1] William R. Holmes,[2] Jean P. Thiery,[4,5] Rodney B. Luwor,[3] and Vijay Rajagopal[1,*]
[1]Department of Biomedical Engineering, University of Melbourne, Melbourne, Victoria, Australia; [2]Department of Physics and Astronomy, Vanderbilt University, Nashville, Tennessee; [3]Department of Surgery, The University of Melbourne, The Royal Melbourne Hospital, Melbourne, Victoria, Australia; [4]CNRS Emeritus CNRS UMR 7057 Matter and Complex Systems, University Paris Denis Diderot, Paris, France; and [5]Guangzhou Laboratory, Guangzhou, 510320, China

ABSTRACT Adherens junctions physically link two cells at their contact interface via extracellular binding between cadherin molecules and intracellular interactions between cadherins and the actin cytoskeleton. Cadherin and actomyosin cytoskeletal dynamics are regulated reciprocally by mechanical and chemical signals, which subsequently determine the strength of cell-cell adhesions and the emergent organization and stiffness of the tissues they form. However, an understanding of the integrated system is lacking. We present a new mechanistic computational model of intercellular junction maturation in a cell doublet to investigate the mechanochemical cross talk that regulates adherens junction formation and homeostasis. The model couples a two-dimensional lattice-based simulation of cadherin dynamics with a reaction-diffusion representation of the reorganising actomyosin network through its regulation by Rho signalling at the intracellular junction. We demonstrate that local immobilization of cadherin induces cluster formation in a *cis*-less-dependent manner. We then recapitulate the process of cell-cell contact formation. Our model suggests that cortical tension applied on the contact rim can explain the ring distribution of cadherin and actin filaments (F-actin) on the cell-cell contact of the cell doublet. Furthermore, we propose and test the hypothesis that cadherin and F-actin interact like a positive feedback loop, which is necessary for formation of the ring structure. Different patterns of cadherin distribution were observed as an emergent property of disturbances of this positive feedback loop. We discuss these findings in light of available experimental observations on underlying mechanisms related to cadherin/F-actin binding and the mechanical environment.

SIGNIFICANCE Formation, maintenance, and disassembly of adherens junctions is fundamental for organ development, tissue integrity, as well as tissue function. Cadherins and actin filaments (F-actin) are two major players in adherens junctions. Although it is well known that cadherins and F-actin affect each other, how they work together to form and maintain intercellular contact is unclear. Using a novel mechanochemical model of cadherin and F-actin remodeling, we demonstrate that a positive feedback loop between cadherins and F-actin allows them to stabilize each other locally. Mechanical and chemical stimuli applied to cell adhesion change cadherin and F-actin distribution by consolidating or interrupting the feedback loop locally. Our study mechanistically illustrates the mechanism of cadherin patterning at cell-cell junctions.

INTRODUCTION

Cadherin is a transmembrane protein at adherens junctions (AJs), which physically link adjacent cells through *trans* and *cis* extracellular binding and cytoplasmic interactions with the actin cytoskeleton. Cadherin-based adhesion junctions are also key regulators of morphogenesis, tumorigenesis, and cancer progression (1,2). Because the adhesive activity of individual cadherin molecules is negligible, cadherin clustering is necessary for AJ assembly during the process of cell-cell junction formation (3,4). Experiments using optical tweezers have suggested that the actin cytoskeleton plays a crucial role in regulating cadherin clustering through corralling and tethering (5). Moreover, the actin cortex can transmit intracellular contractility and extracellular stresses to AJs, which results in cadherin redistribution and changes in the cadherin turnover rate (6,7). However, cadherin ligation can also simultaneously regulate actin network dynamics and contractility via Rho-Rac signaling pathways (8–10). How does the reciprocity between cadherin and actin drive cell-cell junction formation? How does the cross talk between cadherin and actin dynamics help maintain

Submitted July 7, 2021, and accepted for publication January 10, 2022.
*Correspondence: vijay.rajagopal@unimelb.edu.au
Editor: Padmini Rangamani.
https://doi.org/10.1016/j.bpj.2022.01.006

contact integrity? This study aims to address these two questions in a quantitative, mechanistic manner. We review key experimental observations of the cross-talk between cadherin and the actin cytoskeleton that we will investigate further in this study.

The actin cytoskeleton acts as a scaffold, guiding cadherin clustering via cadherin/actin filaments (F-actin) adaptors such as vinculin and α-catenin (3). Deletion of cadherin's cytoplasmic region and knockdown of α-catenin lead to transient and unstable clustering (7), impairing contact stability. In contrast, jasplakinolide-induced actin polymerization can stabilize cadherin clusters (11). In addition to tethering cadherin, previous studies have suggested that cadherin diffusion is confined by F-actin (5,12), with a mesh size of 50–200 μm (13). The finding was confirmed by a computational study that predicted a decrease in cadherin displacement and cluster size when F-actin acts as a movement barrier (14). In this study, we use a biophysics-based model to investigate the effect of cadherin-actin interactions on cadherin organization at the contact interface.

In addition to physically linking to cadherin and regulating cadherin diffusion, the actin cytoskeleton transmits intracellular and extracellular forces to AJs and vice versa (15–17). The protein complex composed of F-actin, cadherin, and cadherin/F-actin adaptors is always under tension. The tension is approximately 2–5 picoNewtons (pN) under resting conditions and rises to ∼50 pN under stressed conditions (18). Interestingly, cellular contractility is necessary to maintain AJs. Inhibition of cellular contractility leads to a decrease in cadherin-based cell adhesiveness (16,19,20). Force-sensitive bonds around cadherin grant AJs high resilience in response to mechanical stimuli. For example, as a member of the cadherin-catenin complex (21), the autoinhibitory α-catenin can be unfolded with a tension of 5 pN (22). The bond between α-catenin and F-actin acts as a catch-slip bond whose lifetime is maximized at around 8 pN (21). We incorporate a simple force-balance equation to our model of cadherin-actin dynamics to investigate the mechanobiology of AJ formation and maturation.

On the other hand, cadherin can also regulate the dynamics and contractility of the actin cytoskeleton. Upon initial cell-cell contact, cadherin ligation activates a series of signaling cascades (10), such as Rho GTPase. Among the Rho GTPase family, regulation of Rac by cadherin *trans*-dimerization through the c-Src-Rap1-PI3-K-Vav2 signaling pathway is well established (8). Contact-induced Rac activates actin nucleation and polymerization via the downstream effector arp2/3. In addition, experiments suggest that Rho, a regulator of myosin, which contracts and stiffens the actin network, is downregulated by cadherin ligation through the cross talk between Rho and Rac in a p190RhoGAP-dependent manner (23). We study the interactions between these signaling pathways to determine key features of AJ formation.

Actin and cadherin, two main players in AJ formation and maintenance, are regulated by the dynamics of each other through mechanical and biochemical signals. Biophysics-based computational models enable systematic dissection of different interacting mechanisms, but computational studies of AJ formation to date have investigated the dynamics of cadherin or actin separately (14,24–27). Furthermore, the limited number of cadherin molecules (<200 molecules) simulated in these models and the short time scales (<10 s) prevent investigation of contact formation and rearrangement. We addressed these limitations by developing a new computational model that integrates cadherin clustering, cadherin/F-actin binding, RhoA/Rac signaling pathways, and actin cortex contractility to recapitulate the whole process of cell-cell contact formation and rearrangement. Our systematic analysis of the model predictions suggests a system where actin and cadherin regulate each other in a positive feedback loop. Internal or external stimuli modulate this feedback loop to reinforce the junction locally. On the other hand, inhibition or breakage of the loop leads to failure of contact maturation. The positive feedback loop ensures strength and resilience of the cell-cell junction.

A new computational model of cell-cell adhesion formation

A lattice-based model of cadherin

A lattice-based model is adapted from a previous computational study (24) to simulate cadherin interactions and clustering on the two opposing cell membranes. The two opposing cell membranes are represented by two square surfaces with periodic boundaries. As shown in Fig. 1 , *A* and *B*, the side length of each lattice site is 7 nm, which is the spacing between E-cadherins in the crystal structure (28,29). Columns A and B represent monomers on membranes 1 and 2, respectively (Fig. 1 *A*), and D represents a *trans* dimer, $A + B \rightleftarrows D$.

Within each time step, all mobile cadherins attempt a movement toward one of four nearby neighbor lattices. Double occupancy of one lattice site by two As or two Bs is not allowed. Thus, movement toward an occupied lattice would be rejected in this model framework.

Each particle may also orient toward one of four possible directions available in a lattice structure: north (N), east (E), south (S), and west (W). These orientations represent the orientation of the binding site of a cadherin molecule within the lattice structure. The orientations are tangential to the membrane, not perpendicular.

Within each time step, the binding site orientation is chosen at random for each mobile cadherin. After updating lattice position and binding-site orientation, *trans* and *cis* association and dissociation calculations are performed. A and B must be placed in one lattice site to form a *trans* dimer. As a result, there are four types of monomers on each side: A_N, A_E, A_S, and A_W and B_N, B_E, B_S, and B_W (Fig. 1 *B*). Consistent with

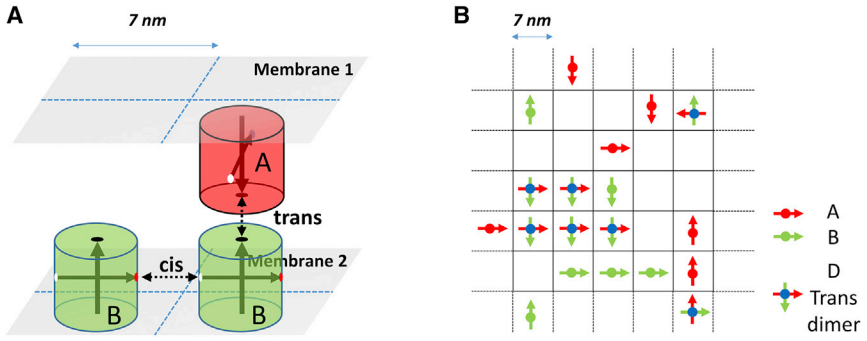

FIGURE 1 Lattice-based model of cadherin dynamics. (*A*) Schematic of cadherin *trans* and *cis* interactions on the lattice-based model. (*B*) The 2D field is composed of square lattices, representing the contact area of a cell doublet. Each lattice can only be occupied by one monomer from each cell. Simultaneous occupancy by a monomer A from the upper membrane (red arrow) and a monomer B from the bottom membrane (green arrow) is necessary for formation of a *trans* dimer (blue dot). Monomers from the same surface can interact with each other through *cis* interaction.

the crystal structure, a *trans* dimer can only be formed by an A and a B, where B's orientation is rotated clockwise by 90° relative to A's orientation (e.g., $D_{NE} = A_N - B_E$). Two monomers on the same surface can interact via their *cis* interfaces only when they occupy the nearest-neighbor sites along the same axis; e.g., $A_N - A_N$. A *trans* dimer can only interact with a neighboring *trans* dimer when they have the same orientation; e.g., $D_{NE} - D_{NE}$. Because of the two orthogonally oriented monomers in a dimer, a *trans* dimer can interact with dimers and monomers in both axes. The binding and unbinding probabilities are computed as a function of the binding affinities Δg^0_{trans} or Δg^0_{cis}. Details regarding the computational process can be found in elsewhere (24).

The length of a single time step used in the simulation can be calculated using the following formula, assuming x is 7 nm:

$$\Delta t = \frac{x^2}{\eta D} \tag{1}$$

, where Δt is the time step, x is the distance between two lattices, D is the diffusion coefficient of E-cadherin (25), and η equals 4 for two-dimensional (2D) diffusion.

Reaction-diffusion (RD) model of the actomyosin network and RhoA/Rac signaling

Trans-dimerization of cadherin activates Rac, which then locally induces actin polymerization. Activated Rac inhibits RhoA, which dampens myosin phosphorylation and contractility (Fig. 2 *A*). We incorporated these effects of cadherin on actin polymerization into a minimal RD model of actin cytoskeleton reorganization.

The dynamics of chemical species are solved based on the RD equation:

$$\frac{\partial u_i}{\partial t} = D_i \frac{\partial^2 u_i}{\partial x_j^2} + R(u_i) \tag{2}$$

, where u_i stands for the local concentration of chemical species i, which is a function of time t and distance x_j in dimension j, D_i is the diffusion coefficient of the species, and $R(u_i)$ accounts for all local reaction kinetics of chemical species i.

The partial differential RD equations of chemical reactions on the cell-cell contact were solved using the finite element modelling package, OpenCMISS (30), on a circular simplex triangulated mesh representing the "contact area" with a radius of 0.5 μm (Fig. S6). The processes of mesh building and the details of chemical signals can be found in the supporting material.

Coupling between the lattice-based model and RD model

At the beginning of simulations on the 2D circular domain of the adhesion junction, cadherin monomers are distributed randomly in the lattice-based model, and concentrations of all chemical species are homogeneous in the RD model. Within each time step of the RD model, position and state (*trans*, *cis*, monomer) information of cadherin molecules in the lattice-based model are mapped to the finite element mesh of the RD model. Local concentration of cadherin monomers $[cad]$ and *trans* dimers are then computed and updated within the finite element mesh. As the cadherin monomers in the lattice-based model associate into *trans* dimers, the signaling cascade of RhoA/Rac and the actomyosin network is triggered in the RD model.

Cadherin is immobilized when it is trapped by the actin network and becomes mobile only after the bond dissociates. Experiments showed that newly synthesized cadherin associates with β-catenin in the endoplasmic reticulum, and the protein complex is transported from the endoplasmic reticulum (ER) to the lateral membrane afterward (31,32). The bond between α-catenin and the β-catenin/cadherin complex ($K_d \sim 1$ nM) (33,34) is much stronger than the bond between α-catenin and F-actin ($K_d \sim 1$ μM) (35–37). Thus, we simplified the linker-mediated cadherin-actin binding as direct binding between cadherin and F-actin. The association rate between cadherin and F-actin is set as a constant throughout the simulations.

Because of the force-sensitive nature of the α-catenin/F-actin bond (Figs. S9 and S10), the dissociation rate of cadherin/F-actin bond is calculated as a function of the average link tension λ sustained in each *trans* dimer (Fig. 2 *B*). The cortical tension β, a sustained contraction of the cortical actin cytoskeleton, is set as a constant. Because the actin cytoskeleton reorganizes and the cadherin cluster assembles,

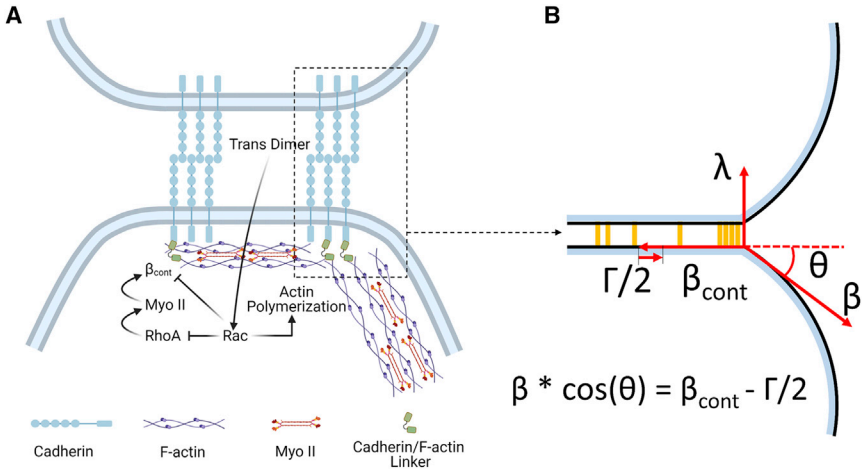

FIGURE 2 Biochemical signaling pathway and mechanical tension in cell adhesion of a cell doublet. (*A*) Upon cell-cell contact, cadherin *trans* dimers upregulate Rac, which works as an upstream regulator of actin polymerization. Rac also inhibits RhoA, myosin, and contact contractility β_{cont} via p190B-RhoGAP. (*B*) Cadherin *trans*-dimerization and clustering lead to an increase in adhesion tension Γ. Assuming a contact cortical tension β, as the actin cortex disassembles on the contact, β_{cont} decreases, whereas the contact angle θ and the linking tension λ sustained in the cadherin-catenin-actin complex increase. The cell membrane is shown in black and the actin cortex in blue. Cadherin *trans* dimers are represented by orange bars between membranes.

contractility from the actin cytoskeleton beneath the contact membrane, βcont, evolves and is computed as a function of activated myosin walking on F-actin $[myo^* - actin^*]$ (see supporting material). Adhesion tension Γ is the product of the number of cadherin *trans* dimers and the *trans* dimer binding energy. Assuming a constant cortical tension β, the link tension λ and dissociation rate of the cadherin/F-actin bond can be computed over time using the force balance equation [Fig. 2 *B*]:

$$\beta = \beta_{cont} + \lambda + \frac{\Gamma}{2} \tag{3}$$

. Further details of the implementation of this mechanical coupling within the model can be found in the supporting material.

RESULTS

Cadherin immobilization leads to clustering

Cadherin clustering is necessary for assembly of AJs. Studies have indicated that the cooperation between *trans* and *cis* interactions can drive cadherin clustering (24). However, by blocking cadherin diffusion and immobilizing cadherin locally, the actin cytoskeleton can induce cluster formation in a *trans*- or *cis*-independent manner (3).

Here we use the lattice-based model of cadherin to investigate the possible roles of actin in cadherin clustering. We run two groups of simulations with a wide range of *trans* and *cis* binding affinities, Δg^0_{trans} and Δg^0_{cis}. In the first set of simulations, cadherin monomers are free to diffuse and interact with each other through *trans* and *cis* on the field composed of 50 × 50 lattice sites with periodic boundaries (Fig. 3 *A*). In contrast, in the second set of simulations, *trans* dimers are immobilized when they form in the central 10 × 10 "immobilization zone" or when they diffuse from the outside to the immobilization zone, labeled by a black square in Fig. 3 *C*.

We analyzed the maximum cluster size in each simulation from two groups. In the first group, in accordance with previous studies (14), intermediate *cis* binding affinity (∼3–6 kBT) allows cadherin molecules to form larger clusters. The finding is consistent with higher cadherin concentrations (Fig. S1).

In the second simulation group, cadherins can form large clusters exclusively in the central immobilization zone, even with a weak *cis* binding affinity (<2 kBT) (Fig. 3, *C* and *D*), which agrees with the experimental observation that cadherin binding to F-actin drives cadherin clustering in a *cis*-independent manner (3). Furthermore, as shown in Fig. 3, *A* and *B*, cadherin molecules are not able to form large clusters with a weak *cis* binding affinity. This finding suggests that immobilization of cadherin drives clustering locally by decreasing the requirement of *cis* binding affinity.

Cortical tension stimulates formation of cadherin and actin ring-like distribution

The actin cortex is expressed uniformly underneath the cell membrane before two cells form an adhesion. During cell-cell contact formation, the actin cortex at the contact center diminishes gradually. Actin and adhesion molecules, including cadherin, β-catenin, and α-catenin, accumulate at the contact rim, forming a ring-like distribution (7,38–40). With our simulation prediction that cadherin immobilization induces clustering locally and the fact that α-catenin/F-actin bond lifetime is sensitive to force (21), we propose that the vertical component of cortical tension applied on the contact edge could be the reason for the cortex reduction on the contact center and ring formation on the contact edge.

To test this hypothesis, we constructed a 2 × 2 μm lattice field composed of 286 × 286 lattices with periodic boundaries. The central circular region of the lattice-based model with a diameter of 1 μm represents the cell-cell "contact area." The region outside of the "contact area" is referred

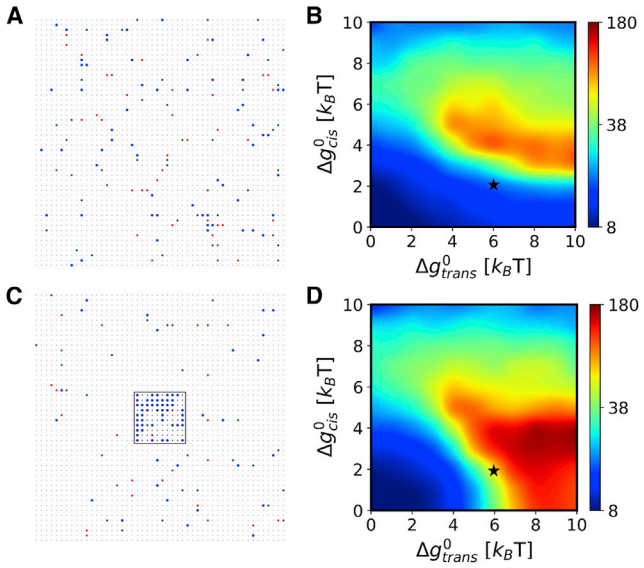

FIGURE 3 Cadherin dynamics were simulated on a region composed of 50 × 50 lattice sites. (*A–D*) With the periodic boundaries, cadherin can diffuse across the boundaries. The monomer concentration is 0.04 on each side. The snapshots in (*A*) and (*C*) were taken when the maximum cluster appears in the simulation with $\Delta g^0_{trans} = 6k_BT$ and $\Delta g^0_{cis} = 2k_BT$. The maximum cluster size from these simulations are labeled by black stars in (*B* and *D*). Blue dots represent *trans* dimers, and red and green dots represent cadherin monomers located on the two opposite surfaces. Heatmaps in (*B*) and (*D*) show the maximum cluster size in each simulation with a wide range of Δg^0_{trans} and Δg^0_{cis}, from 0–10 kBT. The cluster size is calculated by counting the number of cadherin molecules in each cluster. Each data point represents the mean value of the maximum cluster size of five simulations. In (*A*) and (*B*), *trans* dimers can be formed everywhere. All cadherin monomers and *trans* dimers can diffuse freely on all lattices. In (*C*) and (*D*), *trans* dimers can be formed everywhere but will be immobilized when they are in the central 10 × 10 lattice "immobilization trap" (black square) and can only leave after the *trans* dimer dissembles.

to as the "contact-free area," which is not in contact with the opposing cell. *trans*-dimerization is only allowed on the contact area. Movements of *trans* dimers toward the "contact-free area" are rejected. The cadherin concentration $[cad]$ was set to 0.04 or 800 monomers/μm^2 on each surface. The cortical tension β was set to 4,000 pN/μm. The affinities of *trans* and *cis* interactions were set to 6 kBT and 2 kBT, respectively.

The lateral edges of the two cells in contact exert an out-of-contact-plane cortical tension β, solely on the "contact edge". The edge was represented as a ring with a width of 0.05 μm on the rim of the "contact area" and is equivalent to the thickness of the cortex. In contrast to the "contact edge," the central circle with a radius of 0.45 μm is called the "contact center." The dissociation rate between *trans* dimers on the "contact edge" and F-actin is calculated as a function of the force sustained in each dimer (see the supporting material for more details). The initial contact contractility βcont was set to be the same as the cortical tension β at the basal contact surface. Accordingly, the initial contact angle θ was also set to 0°.

Fig. 4 illustrates the model-predicted changes in the spatial distribution of actin and cadherin through the contact maturation process. As the simulation begins, cadherin monomers from two opposing surfaces associate into *trans* dimers. Rac upregulated by *trans* dimers initiates actin polymerization and inhibits βcont through downregulation of RhoA (Fig. 2 *A*). As the βcont decreases, the contact angle θ increases (Fig. 2 *B*) to maintain force balance. The newly formed *trans* dimers experience a large force transmitted from the cortical tension (Fig. 4 *B*). Because *trans*-dimerization can only take place on the "contact area," the "contact area" serves as a *trans* dimer diffusion trap, as suggested in a previous study (24). As cadherin from the "contact-free area" diffuses to the "contact area," cadherin concentration on the "contact center" increases and converges in the first 25 s [Fig. 4 *D*]. Along with the concentration increase, cadherin monomers start to assemble into clusters on the contact through *trans* and *cis* interactions (Fig. 4 *D*).

Fig. 4 *C* illustrates the changing properties of cadherin clusters during the maturation process. In the first stage, although the contact angle increases and cadherin molecules aggregate to the contact, cadherin clusters are small and unstable (Fig. 4 *A*). Actin is distributed homogeneously on the contact. As the contact angle increases, the lifetime of the cadherin/actin bond increases in response to the tension sustained in the bond, immobilizing cadherin molecules locally on the contact edge. Translocation of cadherin molecules to the contact edge enables formation of larger and more stable clusters locally as more cadherin molecules associate with each other through *cis* binding (Fig. 4 *C*), which strengthens the cell-cell contact. Cadherin accumulation on the contact edge then stimulates actin polymerization locally through Rac, which indirectly leads to actin depletion on the contact center. Convergence of tension sustained in *trans* dimers and the accompanying formation of cadherin and the actin ring-like structure indicate maturation of cell-cell contact.

With the cortical tension-stimulated longer cadherin/F-actin lifetime on the contact edge, cadherin molecules accumulate locally. A locally higher cadherin concentration on the contact edge upregulates *trans*-dimerization and induces actin polymerization via Rac. Actin accumulation on the contact edge competes for the limited actin pool and leads indirectly to diminishment of the actin cortex on the contact center.

The positive feedback loop between cadherin and F-actin is essential for ring formation

We conducted a parameter sensitivity analysis in our model framework to determine how ring formation is governed by the interactions between cadherin and actin. We simulated adhesion formation over a wide range of values of the *trans* dimer-stimulated Rac activation rate, $k_{Rac}^{on(trans)}$, and the binding rate between cadherin and F-actin, $k_{cad/Factin}^{on}$ (Fig. 5 *A*).

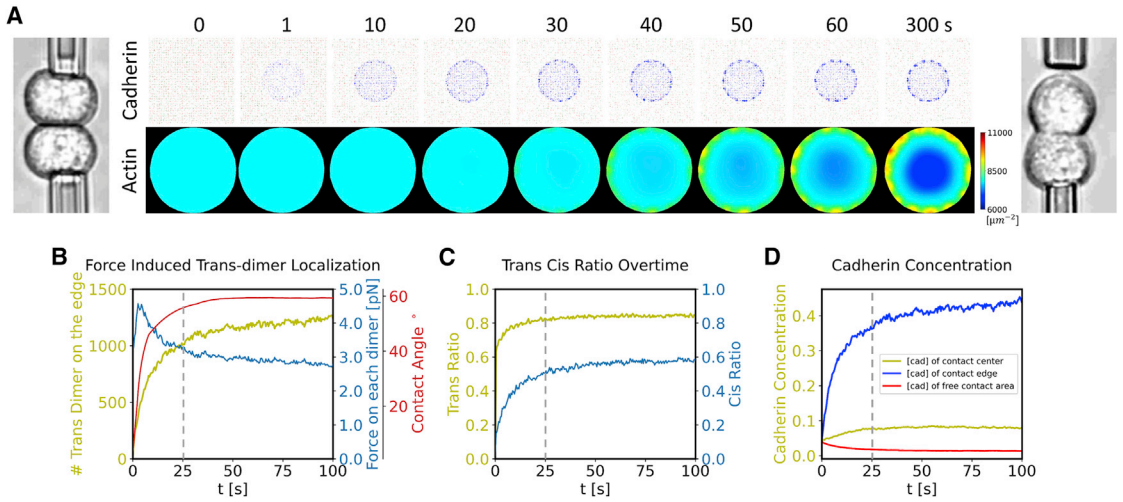

FIGURE 4 The process of cell-cell contact formation. (*A*) Serial snapshots of the lattice-based model of cadherin and RD model of actin (sum of G-actin (actin) and F-actin (actin*)). The model replicates the maturation process of the cell-cell contact when two cells are brought to each other. Photos on the two sides show the experiment where two cells were brought into contact using micropipettes (41). Two cells were gently held in contact using micropippettes for 4 min. The left image shows the cells at the start of the experiment and the right image shows the adhered cells after 4 min.. (*B*) Development of the contact in the first 100 s. *trans* dimers translocate and form on the contact edge to resist the challenge from cortical tension as the contact angle increases. Force sustained in each cad *trans* dimer decreases as more cadherins locate on the contact edge. (*C*) Ratios of monomers on the contact area that are involved in *trans* and *cis* interactions in the first 100 s. (*D*) The concentration of cadherin on the contact center, contact edge, and free contact area in the first 100 s. Cadherin/F-actin binding rate, 10^{-3} μm^2 s^{-1}; Rac activation rate by cadherin *trans* dimer, 10^{-5} μm^2 s^{-1} *cortical tension* $\beta = 4000\,pN/\mu m$; $[cad] = 0.04$; $\Delta g^0_{trans} = 6k_BT$; $\Delta g^0_{cis} = 2k_BT$.

The level of Rac governs actin polymerization, whereas the cadherin/F-actin binding rate determines the possibility that cadherin is immobilized by F-actin.

As we increase $k^{on}_{cad/Factin}$, cadherin density on the "contact area" increases, suggesting that cadherin molecules are trapped by actin after they translocate from the "contact-free area" into the "contact area" (Fig. 5 *B*). Moreover, accumulation of cadherin molecules on the "contact area" enables more frequent *trans* and *cis* interactions (Fig. 5, *D* and *E*).

However, with a low Rac activation rate, cadherin *trans* dimers cannot properly stimulate actin polymerization locally. Clusters formed by cadherins without actin binding sites are transient and unstable, as shown previously in experiments (7). Without the support of actin, cortical tension failed to stimulate cadherin accumulation on the contact edge to form stable clusters (Fig. 5, *A* and *C*).

Based on our findings, we propose that a positive feedback loop exists between cadherin and actin interactions at adherens junctions. The positive feedback loop is initiated by cadherin *trans*-dimerization induced actin local polymerization, which leads to actin tethering induced cadherin local immobilization and accumulation (Fig. 6). Either a low Rac activation rate or a low cadherin/F-actin binding rate inhibits this positive feedback loop on the whole "contact area," leading to failure of contact formation. By increasing the cadherin/F-actin binding lifetime at the contact edge, cortical tension further activates the positive feedback loop exclusively on the contact edge, which differentiates the contact edge from the contact center and induces formation of the ring-like structure.

Disturbance of the cadherin F-actin positive feedback loop results in cadherin redistribution

With the finding that cortical tension stimulates the positive feedback loop on the contact edge, we further propose that inhibition or stimulation of any components in the positive feedback loop can lead to rearrangement of cadherin and actin on a mature contact. A recent experiment showed that cyclical stretching on one side of a cell doublet can locally stimulate actin and cadherin accumulation (38) (Fig. 7 *B*). As shown in the schematic in Fig 7 *B*, because of external stresses induced by hydrodynamic forces around the cell doublet, the tension sustained in the *trans* dimers should be much larger than the static state.

Because we know that the X-dimer, an intermediate during cadherin *trans*-dimerization, is force sensitive, the lifetime of the X-dimer is increased by several times when the force sustained in each X-dimer is around 30 pN (42). We hypothesize that the higher binding affinity on the stretched side (right side) can upregulate the activity of the positive feedback loop.

To test this hypothesis, after 100 s of the initial contact maturation, we cyclically varied the *trans* dimer affinity Δg^0_{trans} on the right contact edge between 6 and 8 kBT with a frequency of 1 Hz and maintained Δg^0_{trans} at all other areas to be 6 kBT. After the initial contact maturation

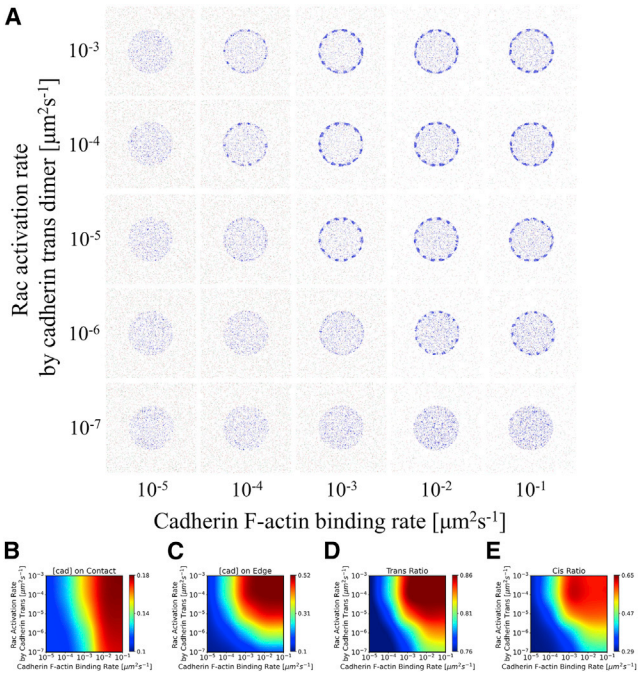

FIGURE 5 The positive feedback loop between cadherin and F-actin is essential for ring formation. (*A*) Snapshots of the cadherin lattice-based model at 300 s. (*B*) Cadherin concentration on the whole contact. (*C*) Cadherin concentration on the contact edge. (*D* and *E*) Ratios of monomers on the contact area that are involved in *trans* and *cis* interactions, respectively. (*B–E*) Average of data in 200–300 s. For all simulations, cortical tension $\lambda = 4{,}000$ pN/μm, $[cad] = 0.04$, $\Delta g^0_{trans} = 6\ k_BT$, $\Delta g^0_{cis} = 2\ k_BT$.

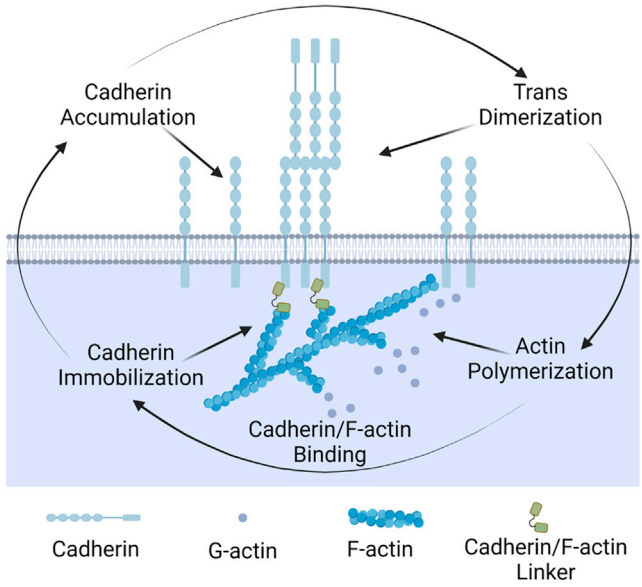

FIGURE 6 The positive feedback loop between F-actin and cadherin. Cadherin *trans*-dimerization leads to actin polymerization in a Rac-dependent manner. F-actin immobilizes cadherin locally through cadherin/F-actin linkers, such as α-catenin and vinculin, leading to cadherin local accumulation. *trans* and *cis* interactions happen more frequently because of local cadherin accumulation, resulting in cadherin clustering.

in the first 100 s, cadherins and actin gradually accumulated at the right contact edge (Fig. 7 *A*, Movie S1). We analyzed the cadherin intensity change, ΔI, before (60–100 s) and after (260–300 s) application of asymmetric *trans* affinity on the contact edge. The ratio between ΔI on the left and right rim, $\Delta I_R/\Delta I_L$, clearly demonstrated that spatially varying the *trans* dimer affinity (induced by spatially varying external mechanical forces) could induce asymmetric distribution of cadherin and actin (normal actin polymerization bars in Fig. 7 *C*). We further tested this proposal by applying an asymmetric actin turnover rate and cadherin/actin dissociation rate on the contact edge (Fig. S5). Our simulation predicted a result that agrees with the experimental observation (7). These results show that disturbance of the positive feedback loop results in cadherin and actin redistribution.

We then investigated what would happen if we blocked the positive feedback loop by significantly increasing actin polymerization to a non-physiological level indiscriminately on the whole "contact area" while keeping a higher *trans* dimer binding affinity on the right contact edge. This simulation is representative of an experimental study that used jasplakinolide to indiscriminately promote actin polymerization (38). The comparison of cadherin intensities with normal actin polymerization and extreme actin polymerization in Fig. 7 *C* indicates that upregulation of actin polymerization indiscriminately on the whole contact area decreases the sensitivity of cadherin to the spatial differences of *trans* dimer affinity, which agrees with the previous experimental observation (38).

DISCUSSION

Key results

Classic cadherin is one of the main players at AJs, whose concentration and distribution are crucial for tissue integrity. Interestingly, experimental studies showed that cadherin cluster size and distribution are not homogeneous on the contact area and can vary dynamically during the process of cell-cell contact development and in response to the external stimulus. Here we developed a parsimonious mechanistic model of the interactions between cadherin and F-actin in cell doublets to study how feedback between the two influences the dynamic distribution of cadherin.

The binding affinity of a *cis* interaction is hard to measure because of the weak nature of the bond. It is estimated that the binding affinity of a *cis* interaction is within a biologically reasonable range of 1–10 mM (25). However, previous computational models have suggested that a high *cis* binding affinity (K_D^{cis}, ~100 μM; Δg^0_{cis}, ~ 3.5 kBT) is required for cluster formation (14,24). By introducing an immobilization zone on the lattice-based field to mimic the effect of actin tethering, we show that cadherin molecules can aggregate into clusters locally in a *cis*-independent manner (Fig. 3),

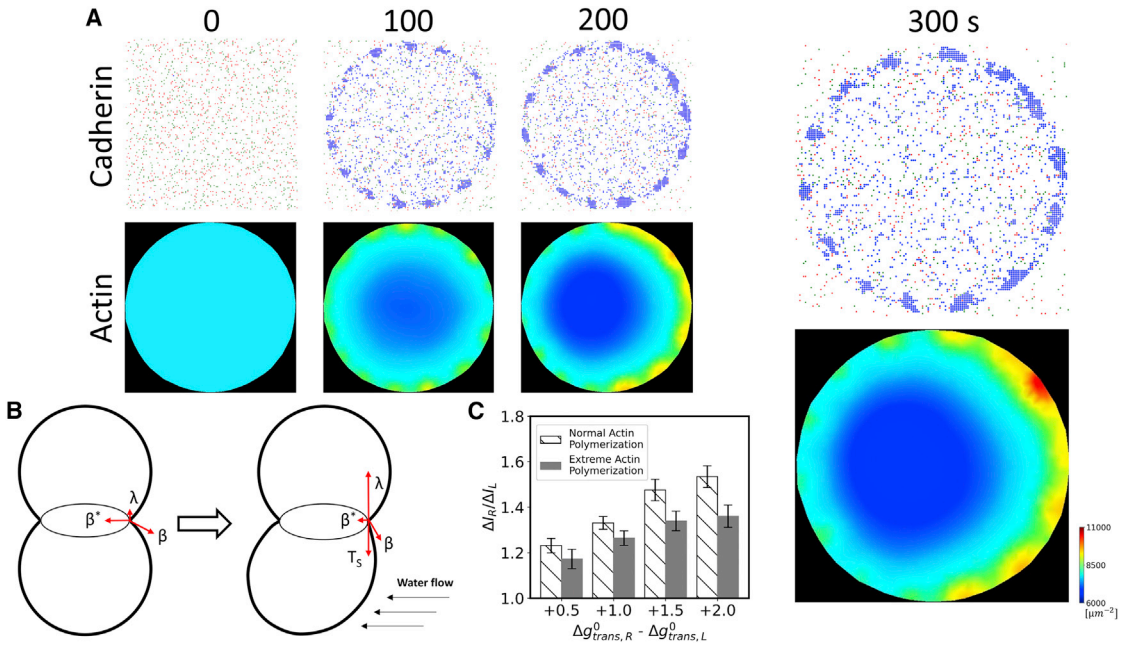

FIGURE 7 Disturbance of the cadherin F-actin positive feedback loop results in cadherin redistribution. (*A*) Serial snapshots of the lattice-based model of cadherin (contact area) and RD model of actin (sum of G-actin (actin) and F-actin (actin*)). The model replicates the process of cadherin and F-actin redistribution on a mature cell-cell contact. The *trans* dimer affinity Δg^0_{trans} was brought up to 8 kBT cyclically with a frequency of 1 Hz after 100 s on the right contact edge and kept at 6 kBT at all other places. (*B*) Schematic of the cell-cell doublet experiment (38). Cyclical water flow introduces external stresses that challenge the cell adhesion with a higher linking tension λ. (*C*) The mean ratios between cadherin concentration change on the right side and left side of the contact rim (ΔI, relative concentration increase). Each column represents the mean value from five simulations. Error bars show the std. Δg^0_{trans} on the right side of the contact rim is increased cyclically to 6.5, 7.0, 7.5, and 8.0 kBT, respectively. Cadherin/F-actin binding rate, 0.5×10^{-3} μm^2 s^{-1}; Rac activation rate by cadherin *trans* dimer, 0.5×10^{-5} μm^2 s^{-1}; cortical tension $\lambda = 4000$ pN/μm, [cad] $= 0.04$; $\Delta g^0_{trans} = 6\ k_BT$; $\Delta g^0_{cis} = 2\ k_BT$.

agreeing with experimental results that demonstrated the existence of cadherin clusters with inactivated *cis* interactions.

In the cell doublet experiment, E-cadherin and F-actin are homogeneous on the cell-cell contact at the initial stage of contact formation but diminish in the contact center as the contact matures, which is, at least in part, a direct result of cadherin-activated signaling cascades (43). A possible mechanism has been proposed where α-catenin competes with Arp2/3 for the actin binding site, inhibiting actin polymerization on the cell-cell contact (44). Apart from that, the distance between cadherin molecules from the opposing membranes might prevent *trans*-dimerization. Membrane curvature driven by membrane fluctuation, cell protrusions facilitated by filopodia and lamellipodia, and size differences of other membrane proteins (14,45) could also lead to inhomogeneous cadherin distribution at the intercellular contact. Another experiment showed that, as two cells approach, Rac1 is prominent at the contact edge, which induces the lamellipodia in this area (46). The lamellipodia on the contact edge might push the membrane into proximity and induce cadherin accumulation solely on the contact edge. The actin network exhibits different morphologies between the early phases of contact formation and the mature contact. The Arp2/3-dependent branching network and the formin mDia1-dependent F-actin bundle formation compete for the actin pool, which dominates the early and later phases, respectively (47–49).

To simulate the process of cell-cell contact formation, we incorporated a parsimonious representation of signaling pathways of the Rho family to the lattice-based model of cadherin dynamics. In Fig. 4, we showed that, as soon as the simulation starts, cadherin molecules move rapidly from the free contact region to the contact region, increasing the concentration of cadherin on the contact region. This mechanism is referred to as a *trans* dimer "diffusion trap" (24). In Fig. S2, we show that the *trans* dimer diffusion trap and cadherin immobilization can induce cadherin accumulation on the cell-cell contact. Our results show that the longer lifetime of the cadherin/F-actin binding induced by the cortical tension can lead to cadherin accumulation on the contact edge because of the locally lower diffusivity. Actin polymerization induced by cadherin *trans*-dimerization on the contact edge further stabilizes the newly formed cadherin clusters. This simulation result agrees with the experimental finding that jasplakinolide-induced actin polymerization can stabilize cadherin clusters (11). We obtained similar results with other sets of *trans* and *cis* binding affinities (Fig. S4). The simulation results in Fig. S3 also further demonstrate the necessity of cortical tension and cadherin concentration for cadherin accumulation on the contact edge. All of these effects of F-actin protrusion, competition between α-catenin and Arp2/3, or competition between formin and Arp2/3 might be interpreted as a singular cause of the ring distribution. But it is most likely that these

mechanisms function simultaneously, including the one suggested by our model: the cortical tension-induced longer cadherin/F-actin lifetime locally upregulates the positive feedback loop between cadherin and F-actin.

Through this computational investigation, we identified that the crux of cadherin patterning at AJs is spatially varying binding affinity and mobility of cadherin molecules on the cell membrane. For example, in Fig. 3, we show that local immobilization induces local cadherin clustering; in Fig. 4, we demonstrate that cortical tension applied on the contact edge leads to cadherin accumulation by increasing the binding lifetime between cadherin and F-actin; and in Fig. 7, our finding illustrates that locally higher *trans* binding affinity results in asymmetrical cadherin distribution on the contact edge. Moreover, these spatial differences are strengthened by the positive feedback loop between cadherin and actin. Disruption of the positive feedback loop weakens the effect of spatial differences (Fig. 7 *C*). Thus, it would be interesting to investigate the effect of other factors on cadherin patterning; for instance, locally different concentrations and activation states of cadherin/actin adaptors.

Opportunities for model extensions to advance the mechanistic understanding of cell-cell adhesions

The model we present here treats the intercellular junction as two flat and static surfaces. Although this is sufficient to represent the condition in the cell-cell doublet experiments to which the model was compared, the experimental condition may not represent true physiological conditions found *in vivo*. However, the model and the experimental conditions we simulated capture salient interactions between key components of the AJ machinery.

Cell-cell adhesion formation involves dynamic interactions between membrane protrusions between the two adjacent cells. Endo- and exocytosis are also known to play important roles in cadherin turnover (6). These data are currently unavailable for the experiments we studied with our new model. In the future, detailed measurements of these molecular events could be incorporated into our model framework to study their effects.

We used a continuum approximation to simulate remodeling of the actin cytoskeleton. Actin cytoskeleton remodeling has been successfully represented previously using RD models (50) and has the advantage of simulating longer timescales and larger fields of view than a typical coarse-grained model of actin cytoskeleton filaments. However, a coarse-grained model of the actin cytoskeleton would be useful to more precisely investigate the corralling effects of actin on cadherin. One could also investigate the effects of actin filament length and turnover on cadherin clustering, which the present model cannot resolve.

Future studies with our model framework should involve more direct connections between the model and experiments so that more quantitative insights can be extracted from the model. Model uncertainty quantification would also benefit from data-informed model parameterization.

Although cortical contractility is assumed to be homogeneous in our simulations, previous studies have identified that they could vary spatially and temporally, such as pulsatile contraction of the actomyosin network (27,51,52). Because AJs are mechanosensitive, explorations of how heterogeneity of cortical contractility affects cadherin clustering and contact maturation could be interesting.

Using mechanistic modeling, we demonstrate a positive feedback loop at cell-cell adhesions from cadherin *trans*-dimerization-induced actin local polymerization to actin tethering-induced cadherin local immobilization and accumulation. Following the concept of the positive feedback loop, our model successfully recapitulates the whole process of cell-cell contact formation of a cell doublet and other experimental observations. Our model suggests that inhibition or stimulation of any components in the positive feedback loop can locally change the activity level and induce cadherin and actin reorganization. We believe that the positive feedback loop ensures the strength and stability of the cell-cell contact.

DATA AND CODE AVAILABILITY

The model used in this work and the code used for analysis are shared on GitHub. https://github.com/CellSMB/cell_cell_adhesion.

SUPPORTING MATERIAL

Supporting material can be found online at https://doi.org/10.1016/j.bpj.2022.01.006.

AUTHOR CONTRIBUTIONS

Q.Y., V.R., and R.B.L. designed the research. Q.Y. performed the research. Q.Y. and V.R. analyzed data. Q.Y., W.R.H., J.P.T., and V.R. wrote the paper.

ACKNOWLEDGMENTS

We thank Jiawen Chen, Xumei Gao, and Virgile Viasnoff for helpful discussions.

REFERENCES

1. Song, Y., M. Ye, …, X. Zhu. 2019. Targeting E-cadherin expression with small molecules for digestive cancer treatment. *Am. J. Transl. Res.* 11:3932–3944.
2. Yu, W., L. Yang, …, Y. Zhang. 2019. Cadherin signaling in cancer: its functions and role as a therapeutic target. *Front. Oncol.* 9:989. https://doi.org/10.3389/fonc.2019.00989.
3. Hong, S., R. B. Troyanovsky, and S. M. Troyanovsky. 2013. Binding to F-actin guides cadherin cluster assembly, stability, and movement. *J. Cell Biol.* 201:131–143. https://doi.org/10.1083/jcb.201211054.
4. Baumgartner, W., P. Hinterdorfer, …, D. Drenckhahn. 2000. Cadherin interaction probed by atomic force microscopy. *Proc. Natl. Acad. Sci. U S A.* 97:4005–4010. https://doi.org/10.1073/pnas.070052697.

5. Sako, Y., A. Nagafuchi, …, A. Kusumi. 1998. Cytoplasmic regulation of the movement of E-cadherin on the free cell surface as studied by optical tweezers and single particle tracking: corralling and tethering by the membrane skeleton. *J. Cell Biol.* 140:1227–1240. https://doi.org/10.1083/jcb.140.5.1227.
6. de Beco, S., C. Gueudry, …, S. Coscoy. 2009. Endocytosis is required for E-cadherin redistribution at mature adherens junctions. *Proc. Natl. Acad. Sci. U S A.* 106:7010–7015. https://doi.org/10.1073/pnas.0811253106.
7. Engl, W., B. Arasi, …, V. Viasnoff. 2014. Actin dynamics modulate mechanosensitive immobilization of E-cadherin at adherens junctions. *Nat. Cell Biol.* 16:587–594. https://doi.org/10.1038/ncb2973.
8. Fukuyama, T., H. Ogita, …, Y. Takai. 2006. Activation of Rac by cadherin through the c-Src-Rap1-phosphatidylinositol 3-kinase-Vav2 pathway. *Oncogene.* 25:8–19. https://doi.org/10.1038/sj.onc.1209010.
9. Ratheesh, A., R. Priya, and A. S. Yap. 2013. Coordinating Rho and Rac: the regulation of Rho GTPase signaling and cadherin junctions. *Prog. Mol. Biol. Transl. Sci.* 116:49–68. https://doi.org/10.1016/B978-0-12-394311-8.00003-0.
10. Menke, A., and K. Giehl. 2012. Regulation of adherens junctions by Rho GTPases and p120-catenin. *Arch. Biochem. Biophys.* 524:48–55. https://doi.org/10.1016/j.abb.2012.04.019.
11. Indra, I., J. Choi, …, S. M. Troyanovsky. 2018. Spatial and temporal organization of cadherin in punctate adherens junctions. *Proc. Natl. Acad. Sci. U S A.* 115:E4406–E4415. https://doi.org/10.1073/pnas.1720826115.
12. Kusumi, A., K. Suzuki, and K. Koyasako. 1999. Mobility and cytoskeletal interactions of cell adhesion receptors. *Curr. Opin. Cell Biol.* 11:582–590. https://doi.org/10.1016/s0955-0674(99)00020-4.
13. Morone, N., T. Fujiwara, …, A. Kusumi. 2006. Three-dimensional reconstruction of the membrane skeleton at the plasma membrane interface by electron tomography. *J. Cell Biol.* 174:851–862. https://doi.org/10.1083/jcb.200606007.
14. Chen, J., Z. R. Xie, and Y. Wu. 2016. Elucidating the general principles of cell adhesion with a coarse-grained simulation model. *Mol. Biosyst.* 12:205–218. https://doi.org/10.1039/c5mb00612k.
15. Yonemura, S., Y. Wada, …, M. Shibata. 2010. alpha-Catenin as a tension transducer that induces adherens junction development. *Nat. Cell Biol.* 12:533–542. https://doi.org/10.1038/ncb2055.
16. Liu, Z., J. L. Tan, …, C. S. Chen. 2010. Mechanical tugging force regulates the size of cell-cell junctions. *Proc. Natl. Acad. Sci. U S A.* 107:9944–9949. https://doi.org/10.1073/pnas.0914547107.
17. le Duc, Q., Q. Shi, …, J. de Rooij. 2010. Vinculin potentiates E-cadherin mechanosensing and is recruited to actin-anchored sites within adherens junctions in a myosin II-dependent manner. *J. Cell Biol.* 189:1107–1115. https://doi.org/10.1083/jcb.201001149.
18. Charras, G., and A. S. Yap. 2018. Tensile forces and mechanotransduction at cell-cell junctions. *Curr. Biol.* 28:R445–R457. https://doi.org/10.1016/j.cub.2018.02.003.
19. Shewan, A. M., M. Maddugoda, …, A. S. Yap. 2005. Myosin 2 is a key Rho kinase target necessary for the local concentration of E-cadherin at cell-cell contacts. *Mol. Biol. Cell.* 16:4531–4542. https://doi.org/10.1091/mbc.e05-04-0330.
20. Miyake, Y., N. Inoue, …, S. Yonemura. 2006. Actomyosin tension is required for correct recruitment of adherens junction components and zonula occludens formation. *Exp. Cell Res.* 312:1637–1650. https://doi.org/10.1016/j.yexcr.2006.01.031.
21. Buckley, C. D., J. Tan, …, A. R. Dunn. 2014. Cell adhesion. The minimal cadherin-catenin complex binds to actin filaments under force. *Science.* 346:1254211. https://doi.org/10.1126/science.1254211.
22. Yao, M., W. Qiu, …, J. Yan. 2014. Force-dependent conformational switch of alpha-catenin controls vinculin binding. *Nat. Commun.* 5:4525. https://doi.org/10.1038/ncomms5525.
23. Wildenberg, G. A., M. R. Dohn, …, A. B. Reynolds. 2006. p120-catenin and p190RhoGAP regulate cell-cell adhesion by coordinating antagonism between Rac and Rho. *Cell.* 127:1027–1039. https://doi.org/10.1016/j.cell.2006.09.046.
24. Wu, Y., X. Jin, …, A. Ben-Shaul. 2010. Cooperativity between trans and cis interactions in cadherin-mediated junction formation. *Proc. Natl. Acad. Sci. U S A.* 107:17592–17597. https://doi.org/10.1073/pnas.1011247107.
25. Chen, J., J. Newhall, …, Y. Wu. 2016. A computational model for kinetic studies of cadherin binding and clustering. *Biophys. J.* 111:1507–1518. https://doi.org/10.1016/j.bpj.2016.08.038.
26. Thompson, C. J., Z. Su, …, D. K. Schwartz. 2020. Cadherin clusters stabilized by a combination of specific and nonspecific cis-interactions. *bioRxiv* https://doi.org/10.1101/2020.05.22.110015.
27. Yu, Q., J. Li, …, T. Kim. 2018. Balance between force generation and relaxation leads to pulsed contraction of actomyosin networks. *Biophys. J.* 115:2003–2013. https://doi.org/10.1016/j.bpj.2018.10.008.
28. Harrison, O. J., X. Jin, …, B. Honig. 2011. The extracellular architecture of adherens junctions revealed by crystal structures of type I cadherins. *Structure.* 19:244–256. https://doi.org/10.1016/j.str.2010.11.016.
29. Truong Quang, B. A., M. Mani, …, P. F. Lenne. 2013. Principles of E-cadherin supramolecular organization in vivo. *Curr. Biol.* 23:2197–2207. https://doi.org/10.1016/j.cub.2013.09.015.
30. Bradley, C., A. Bowery A, …, P. Hunter. 2011. OpenCMISS: a multi-physics & multi-scale computational infrastructure for the VPH/Physiome project. *Progress in. biophysics and molecular biology.* 107:32–47.
31. Chen, Y. T., D. B. Stewart, and W. J. Nelson. 1999. Coupling assembly of the E-cadherin/beta-catenin complex to efficient endoplasmic reticulum exit and basal-lateral membrane targeting of E-cadherin in polarized MDCK cells. *J. Cell Biol.* 144:687–699.
32. Curtis, M. W., K. R. Johnson, and M. J. Wheelock. 2008. E-cadherin/catenin complexes are formed cotranslationally in the endoplasmic reticulum/Golgi compartments. *Cell Commun. Adhes.* 15:365–378. https://doi.org/10.1080/15419060802460748.
33. Yamada, S., S. Pokutta, …, W. J. Nelson. 2005. Deconstructing the cadherin-catenin-actin complex. *Cell.* 123:889–901. https://doi.org/10.1016/j.cell.2005.09.020.
34. Pokutta, S., H. J. Choi, …, W. I. Weis. 2014. Structural and thermodynamic characterization of cadherin.beta-catenin.alpha-catenin complex formation. *J. Biol. Chem.* 289:13589–13601. https://doi.org/10.1074/jbc.M114.554709.
35. Hansen, S. D., A. V. Kwiatkowski, …, W. J. Nelson. 2013. alphaE-catenin actin-binding domain alters actin filament conformation and regulates binding of nucleation and disassembly factors. *Mol. Biol. Cell.* 24:3710–3720. https://doi.org/10.1091/mbc.E13-07-0388.
36. Miller, P. W., S. Pokutta, …, A. V. Kwiatkowski. 2013. Danio rerio alphaE-catenin is a monomeric F-actin binding protein with distinct properties from Mus musculus alphaE-catenin. *J. Biol. Chem.* 288:22324–22332. https://doi.org/10.1074/jbc.M113.458406.
37. Rimm, D. L., E. R. Koslov, …, J. S. Morrow. 1995. Alpha 1(E)-catenin is an actin-binding and -bundling protein mediating the attachment of F-actin to the membrane adhesion complex. *Proc. Natl. Acad. Sci. U S A.* 92:8813–8817. https://doi.org/10.1073/pnas.92.19.8813.
38. Gao, X., B. R. Acharya, …, V. Viasnoff. 2018. Probing compression versus stretch activated recruitment of cortical actin and apical junction proteins using mechanical stimulations of suspended doublets. *APL Bioeng.* 2:026111. https://doi.org/10.1063/1.5025216.
39. David, R., O. Luu, …, R. Winklbauer. 2014. Tissue cohesion and the mechanics of cell rearrangement. *Development.* 141:3672–3682. https://doi.org/10.1242/dev.104315.
40. Maitre, J. L., H. Berthoumieux, …, C.-P. Heisenberg. 2012. Adhesion functions in cell sorting by mechanically coupling the cortices of adhering cells. *Science.* 338:253–256. https://doi.org/10.1126/science.1225399.
41. Chu, Y. S., W. A. Thomas, …, S. Dufour. 2004. Force measurements in E-cadherin-mediated cell doublets reveal rapid adhesion strengthened by actin cytoskeleton remodeling through Rac and Cdc42. *J. Cell Biol.* 167:1183–1194. https://doi.org/10.1083/jcb.200403043.

42. Manibog, K., H. Li, …, S. Sivasankar. 2014. Resolving the molecular mechanism of cadherin catch bond formation. *Nat. Commun.* 5:3941. https://doi.org/10.1038/ncomms4941.

43. Winklbauer, R. 2015. Cell adhesion strength from cortical tension - an integration of concepts. *J. Cell Sci.* 128:3687–3693. https://doi.org/10.1242/jcs.174623.

44. Drees, F., S. Pokutta, …, W. I. Weis. 2005. Alpha-catenin is a molecular switch that binds E-cadherin-beta-catenin and regulates actin-filament assembly. *Cell.* 123:903–915. https://doi.org/10.1016/j.cell.2005.09.021.

45. Li, J. X. H., V. W. Tang, and W. M. Brieher. 2020. Actin protrusions push at apical junctions to maintain E-cadherin adhesion. *Proc. Natl. Acad. Sci. U S A.* 117:432–438. https://doi.org/10.1073/pnas.1908654117.

46. Yamada, S., and W. J. Nelson. 2007. Localized zones of Rho and Rac activities drive initiation and expansion of epithelial cell-cell adhesion. *J. Cell Biol.* 178:517–527.

47. Rao, M. V., and R. Zaidel-Bar. 2016. Formin-mediated actin polymerization at cell-cell junctions stabilizes E-cadherin and maintains monolayer integrity during wound repair. *Mol. Biol. Cell.* 27:2844–2856. https://doi.org/10.1091/mbc.E16-06-0429.

48. Harris, A. R., A. Daeden, and G. T. Charras. 2014. Formation of adherens junctions leads to the emergence of a tissue-level tension in epithelial monolayers. *J. Cell Sci.* 127:2507–2517. https://doi.org/10.1242/jcs.142349.

49. Carramusa, L., C. Ballestrem, …, A. D. Bershadsky. 2007. Mammalian diaphanous-related formin Dia1 controls the organization of E-cadherin-mediated cell-cell junctions. *J. Cell Sci.* 120:3870–3882. https://doi.org/10.1242/jcs.014365.

50. Zmurchok, C., J. Collette, …, W. R. Holmes. 2020. Membrane tension can enhance adaptation to maintain polarity of migrating cells. *Biophys. J.* 119:1617–1629. https://doi.org/10.1016/j.bpj.2020.08.035.

51. Li, J., T. Biel, …, T. Kim. 2017. Buckling-induced F-actin fragmentation modulates the contraction of active cytoskeletal networks. *Soft Matter.* 13:3213–3220. https://doi.org/10.1039/c6sm02703b.

52. Murrell, M. P., and M. L. Gardel. 2012. F-actin buckling coordinates contractility and severing in a biomimetic actomyosin cortex. *Proc. Natl. Acad. Sci. U S A.* 109:20820–20825. https://doi.org/10.1073/pnas.1214753109.